LA-UR-04-8760

Approved for public release; distribution is unlimited.

Title: MCNP5 FOR PROTON RADIOGRAPHY

Author(s):

H. Grady Hughes, Forrest B. Brown, Jeffrey S. Bull, John T. Goorley, Robert C. Little, Lon-Chang Liu, Stepan G. Mashnik, Richard E. Prael, Elizabeth C. Selcow, Arnold J. Sierk, Jeremy E. Sweezy, John D. Zumbro (LANL, USA)
Nikolai V. Mokhov, Sergei I. Striganov (FNAL, USA)
Konstantin K. Gudima (Inst. Appl. Phys., Moldova)

Submitted to:

American Nuclear Society Topical Meeting - Monte Carlo 2005
Chattanooga, TN, USA
April 17-21, 2005.

The Monte Carlo Method: Versatility Unbounded In A Dynamic Computing World

Chattanooga, Tennessee, April 17–21, 2005, on CD-ROM, American Nuclear Society, LaGrange Park, IL (2005)

MCNP5 FOR PROTON RADIOGRAPHY

H. Grady Hughes, Forrest B. Brown, Jeffrey S. Bull, John T. Goorley, Robert C. Little, Lon-Chang Liu, Stepan G. Mashnik, Richard E. Prael, Elizabeth C. Selcow, Arnold J. Sierk, Jeremy E. Sweezy, John D. Zumbro
Los Alamos National Laboratory
Los Alamos, New Mexico 87545 USA
hgh@lanl.gov; fbrown@lanl.gov; jsbull@lanl.gov; jgoorley@lanl.gov; rcl@lanl.gov; liu@lanl.gov; mashnik@lanl.gov; rep@lanl.gov; selcow@lanl.gov; t2ajs@lanl.gov; jsweezy@lanl.gov; zumbro@lanl.gov

Nikolai V. Mokhov, Sergei I. Striganov
Fermi National Accelerator Laboratory
Batavia IL 60510 USA
mokhov@fnal.gov; strigano@fnal.gov

Konstantin K. Gudima
Institute of Applied Physics
Academy of Science of Moldova, Chisinau

ABSTRACT

The developmental version of MCNP5 has recently been extended to provide for continuous-energy transport of high-energy protons. This enhancement involves the incorporation of several significant new physics models into the code. Multiple Coulomb scattering is treated with an advanced model that takes account of projectile and nuclear target form factors. In the next version, this model will provide a coupled sampling of both angular deflection and collisional energy loss, including straggling. The proton elastic scattering model is also new, based on recent theoretical work. Charged particle transport in the presence of magnetic fields is accomplished either by using transfer maps from the COSY INFINITY code (in void regions) or by using an algorithm adapted from the MARS code (in void regions or in scattering materials). Work is underway to validate and implement the latest versions of the Cascade-Exciton Model and the Los Alamos Quark-Gluon-String Model, which will process inelastic nuclear interactions and generate secondary particles.

Key Words: High-energy transport; MCNP, proton radiography.

1 INTRODUCTION

The use of high-energy proton beams for radiography of thick target objects has recently been the subject of considerable theoretical and experimental work at Los Alamos National Laboratory. In the approach being developed under the auspices of the Proton Radiography Component of the Advanced Radiography Campaign, protons passing through a target object

would be focused by a magnetic lens onto a detector located in an image plane. In support of simulation and computational needs of this program, the developmental version of the MCNP5 Monte Carlo transport code [1] has been extended to provide for continuous-energy transport of high-energy protons.

This extension of MCNP5 has required a variety of new developments in the code. Many aspects of the code's infrastructure have been reviewed, generalized, and modernized to facilitate the straightforward introduction of new particle types and new physics modules. Code packages were either adapted from previous prototypes or newly developed and incorporated to deal with proton stopping power, energy-loss straggling, multiple Coulomb scattering, nuclear elastic scattering, nuclear reaction cross sections, and charged-particle transport in magnetic fields. Future work will include testing and validation of the correlated treatment of multiple Coulomb scattering and straggled energy loss, advanced models to treat nuclear interactions and secondary-particle generation, and extension of the code to lower energy ranges with the use of evaluated nuclear data tables. This paper briefly describes these developments and provides references to additional documentation.

2 PROTON STOPPING POWER

At high energies (above 5.24 MeV) the proton stopping power is based on Bethe theory with density-effect corrections described by Sternheimer and Peierls [2]. Ionization potentials are based on values and interpolation procedures recommended in ICRU Report 37 [3]. Atomic shell and subshell corrections are taken from Janni [4], and alternative models by Bichsel [5], Kjandelwal [6], and Walske [7] are available as options. At low energies (below 1.31 MeV), the stopping power is based on the work of Lindhard [8], as in the SPAR code [9]. An energy-weighted interpolation is used in the intermediate range. For immediate applications to proton radiography, only the high-energy range is significant.

Extensive comparisons [10] have recently been made between results of the MCNP5 stopping power model and published data presented in ICRU Report 49 [11]. The agreement in the range from 4 MeV to 10 GeV is generally within 3%. In the range from 1 MeV to 4 MeV, the disagreement grows to about 6%, and in the range from 1 keV to 1 MeV, disagreements as large as 35% are seen. A subset of these comparisons, for five elements, is shown in Figure 1, below. For the present high-energy applications, this situation is satisfactory. Possible future applications at lower energy may require further development of the stopping power model.

3 MULTIPLE COULOMB SCATTERING AND ENERGY-LOSS STRAGGLING

The new algorithm for modeling multiple Coulomb scattering is based on the separate treatment of "soft" and "hard" interactions. A large number of soft collisions are described using a continuous-scattering approximation; a small number of hard collisions are simulated directly. A new analytical expression for a continuous angular distribution was developed for this purpose. The boundary angle between soft and hard collisions is determined as a function of a step-length providing a possibility for fast and precise simulation.

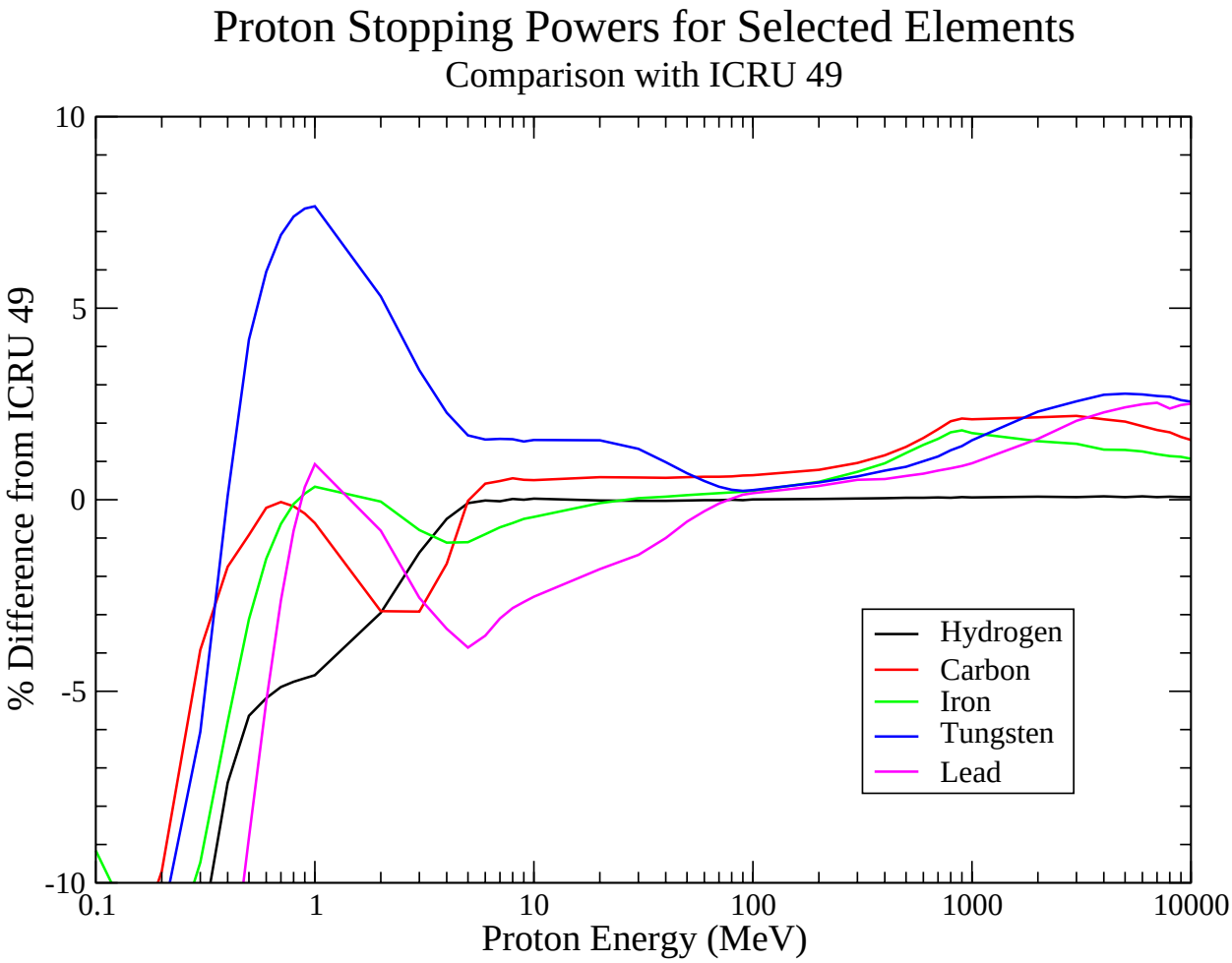

Figure 1. Selected comparisons between the MCNP proton stopping power model and data in ICRU Report 49 (Ref. 11).

Previously in LAHET [12] and in MCNPX [13] a Gaussian model described by Rossi [14] was used for angular deflections. Fig. 2 shows the different behavior of the new model compared with the Gaussian for protons of momentum 24 GeV/c impinging on a thin and a thick tungsten target. In both cases, the new model shows a somewhat enhanced peak and a dramatically slower fall-off at larger angles. This behavior is significant for proton radiography simulations, where the most important features occur at very small angles away from the forward peak.

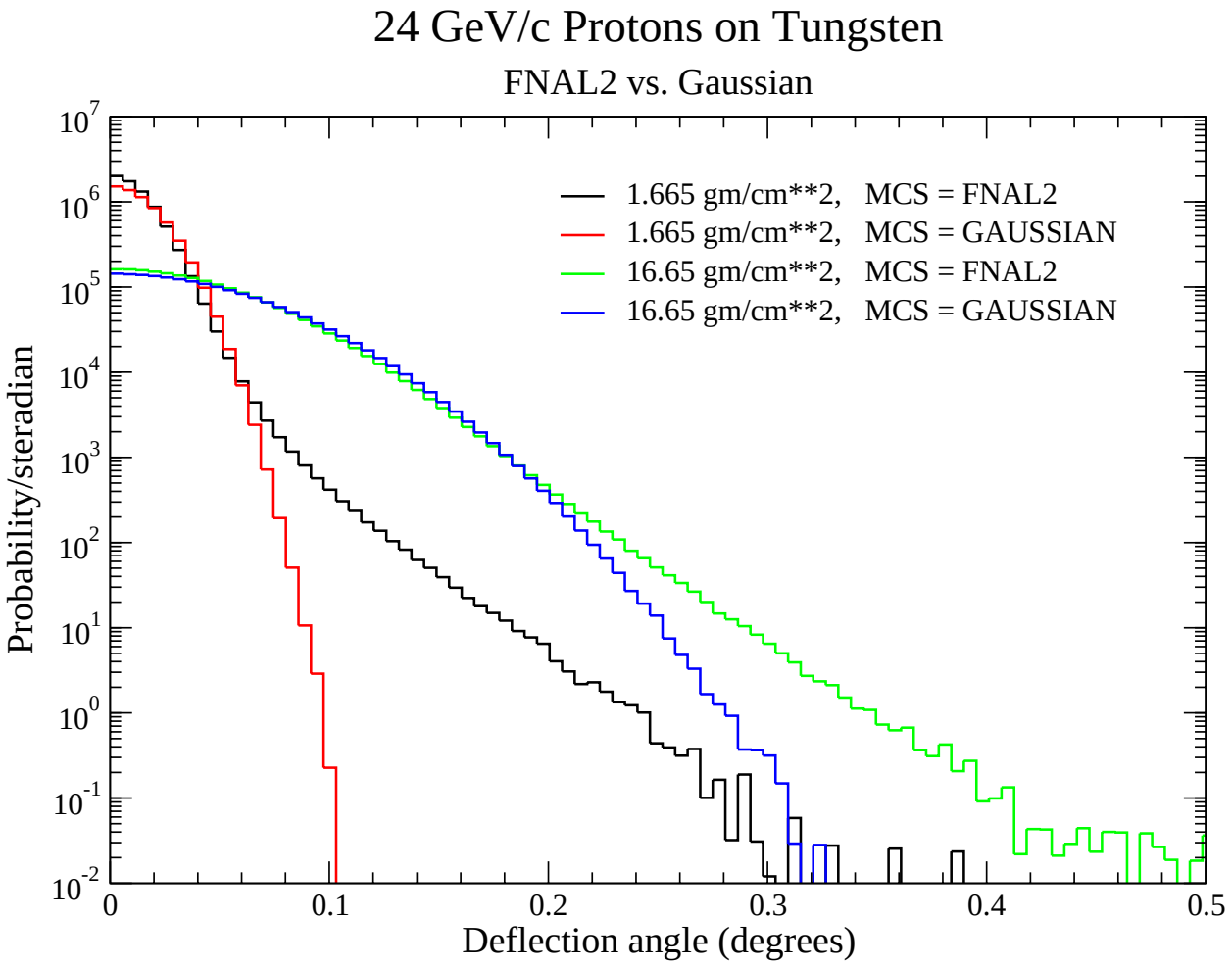

Figure 2. Comparison of the new multiple Coulomb scattering model (FNAL2) with the Gaussian model for 24 GeV/c protons traversing two thicknesses of tungsten.

In the present version of the code, the simulation of energy-loss straggling relies on an unrestricted Vavilov distribution [15], sampled using an algorithm described by Rotondi and Montagna [16]. In the latest version of the new module, however, the straggled energy loss is correlated with the multiple Coulomb scattering of the particle. Hard collisions are sampled taking into account projectile and nuclear target charge distributions and exact kinematics of a projectile-electron interaction. The corresponding energy loss is calculated from the simulated scattering angle. Energy losses in soft projectile-electron collisions are described by a modified Vavilov's function. This complicated function is approximated with high precision using a log-normal distribution. Note that correlation between energy loss and total deflection angle due to scattering on nuclei and electrons is not negligible for low-Z targets.

The new correlated multiple-scattering module is currently undergoing validation and testing. Preliminary results of modeling agree within 1% with analytical calculations of angular and energy-loss distributions. More details of this model are given by Striganov [17].

4 NUCLEAR ELASTIC SCATTERING

A new nuclear elastic scattering model [18] for protons was developed for application to proton radiography at high energies. A processed data library derived from optical model calculations for 23 nuclei between A = 2 and A = 242 and for 47 lab momenta in the range from 1 GeV/c to 50 GeV/c has been created based on optical model elastic differential cross sections; the proton-nucleus elastic differential cross sections were calculated in the framework of eikonal theory. The elastic-scattering data library provides a representation of the angular distribution for scattering in the center of mass. The original cross-section calculations are represented as a sampling distribution for the dimensionless variable X, where $X = q/q_1 = 2p \sin(\theta/2)/q_1$, for center of mass momentum p, momentum transfer q and scattering angle θ, where the variable q_1 is the momentum transfer at the first diffraction minimum. The sampling distribution is interpolated between the tabulated energies and masses.

The sampling method provides an accurate reproduction of the original optical model calculations over a range of seven orders of magnitude in differential cross section. Since the representation separates the sampling distribution for X from the mass and energy dependence of the scattering cross section and q_1, good interpolation is obtained over mass and energy. Validation of the model [18] requires correction of the elastic-scattering component for the additional contributions from multiple Coulomb scattering and incoherent (quasi-elastic) proton scattering. In some cases, the modeling shows deeper diffraction minima than the experimental data, even after corrections are applied. This may be caused by the neglect of Coulomb-nuclear interference. Nevertheless, in general the nuclear elastic-scattering representation provides a good overall description of the process.

For protons of momentum 24 GeV/c traversing a relatively thick tungsten target, Fig. 3 shows the small-angle scattering distribution computed with the new multiple Coulomb scattering model only, with the new elastic-scattering model only, and with both models together. With only the elastic-scattering model, one sees that the forward peak is strongly decreased, but has a delta-function-like feature at zero degrees, representing an unscattered component. The elastic-scattering model also shows the slow decay and the diffraction features reminiscent of the simple black-disk model, but with a faster decay and with smoother, shallower minima. With multiple Coulomb scattering, there are no unscattered particles, so that the forward peak is strongly enhanced, but without the delta-function component. When both multiple Coulomb and elastic scattering are present, the distribution is dominated at small angles by the Coulomb scattering, and at larger angles by the elastic scattering. Even at larger angles, however, the multiple Coulomb scattering plays an important role by smoothing the diffraction peaks and significantly filling in the diffraction minima.

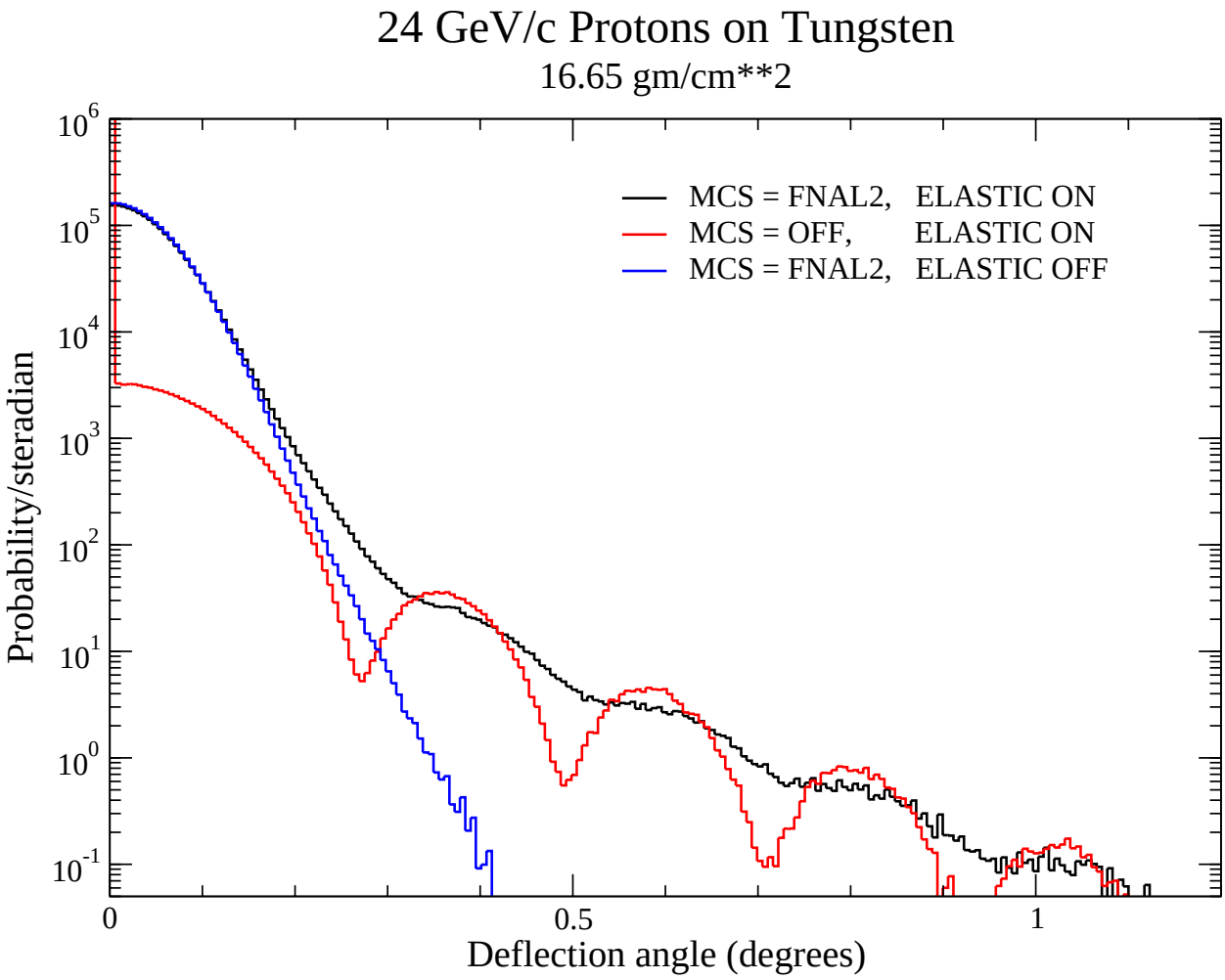

Figure 3. Effects of the multiple Coulomb scattering model (FNAL2), of the elastic-scattering model, and of both processes together.

5 NUCLEAR REACTION CROSS SECTIONS

For proton radiography applications, secondary particles and particles scattered to energies or angles far from their original values can generally be ignored, since the focusing magnets and collimator system will remove such particles from the beam before they reach the image plane. Therefore in Monte Carlo simulations for proton radiography, an inelastic (nuclear reaction) interaction can be treated as absorption or by track weight reduction. Accurate values for the total inelastic cross section are needed so that the attenuation of the beam will be correctly predicted.

In the current version, the MCNP5 high-energy cross-section package accesses the tabulated data of Barashenkov and Polanski [19] as adapted for the MARS code [20-21]. It provides the total, elastic and nonelastic cross sections for nucleons and charged pions interpolated on tabulated target masses from A = 1 to A = 250. The allowed energy range for the charged particles is 1 MeV to 1 TeV; for neutrons, the range is 10 MeV to 1 TeV. In future work, neutron and proton cross sections below 150 MeV will be derived from values in the LA150 nuclear data

tables [22] for the isotopes available in those libraries.

6 TRANSPORT IN MAGNETIC FIELDS

A new feature in MCNP5 allows for transport of heavy charged particles in magnetic fields. Two methods for transporting particles in magnetic fields have been incorporated into the code. The first method utilizes transfer maps generated by the beam optics code COSY INFINITY [23]. Transfer maps are Taylor series expansions of a particle's canonical phase-space coordinates that are used to calculate the changes in these coordinates caused by a charged particle traveling through a magnetic field. When a charged particle enters a cell associated with a transfer map, it is placed at the exit to the cell at a position and with a direction determined from the transfer map and the particle's initial phase space coordinates. Although transfer map methods are quick and accurate, their use is restricted to void regions of a problem's geometry.

The other magnetic field tracking technique utilizes numerical integration techniques similar to other charged particle transport codes. The magnetic field tracking routines were obtained from the high-energy transport code MARS [20-21] and were adapted for use in MCNP5. Three types of magnetic fields are currently built into the code: constant (dipole) fields, hard-edge quadrupole fields, and hard-edge quadrupole fields with edge kicks. The edge-kick model is used to simulate the third-order aberrations due to the effects of the quadrupole fringe fields. These kicks are applicable from the bore region of the magnet out to and including the beam pipe. Studies involving the transport of protons though a magnetic lens system have shown that the edge-kick model results are in close agreement with the transfer map method results.

7 WORK IN PROGRESS

7.1 The Multiple Scattering Model

The final testing of the correlated multiple Coulomb scattering and energy-straggling module is underway. The implications of the correlation in a variety of situations will be explored, and results will be compared with those of previous models.

7.2 Nuclear Interaction Models

The eventual general version of MCNP will include nuclear interaction models to generate secondary particles and to treat the full high-energy cascade. To this end, improved versions of the Cascade-Exciton Model (CEM) [24] code CEM2k+GEM2 and of the Los Alamos Quark-Gluon String Model (LAQGSM) [25] code LAQGSM+GEM2 have been recently developed as event generators [26-29]. The 2003 version of CEM2k+GEM2 (CEM03) is intended to describe nuclear reactions induced by nucleons, pions, and photons at incident energies up to about 5 GeV. The 2003 version of LAQGSM+GEM2 describes reactions induced by both elementary particles and nuclei at energies up to about 1 TeV/nucleon.

The following physics models are contained in the event generators to simulate the different processes involved in various reactions calculable by CEM2k+GEM2 and LAQGSM+GEM2: an improved version of the Dubna intranuclear Cascade Model (DCM), the Quark-Gluon String Model (QGSM), an improved version of the Cascade-Exciton Model (CEM), the Generalized

Evaporation/Fission Model code GEM2 by Furihata, the Fermi break-up model, and a coalescence model. The 2004 versions of the codes, CEM04 and LAQGSM04, comprise significantly improved further versions of the intranuclear cascade model for both CEM2k+GEM2 and LAQGSM+GEM2 and both include also the Statistical Multifragmentation Model (SMM) by Botvina et al., to better describe reactions involving very highly excited nuclei.

We have benchmarked these event generators against most available measured data at projectile energies from 10 MeV/A to 800 GeV/A, and have compared the results with predictions of other current models used by the nuclear community. Our comparisons show that these codes describe a large variety of spallation, fission, and fragmentation reactions quite well and often have a better predictive power than some other available Monte-Carlo codes, thus they can be used as reliable event generators in different applications and in fundamental nuclear research.

7.3 Extension to Low Energies

Evaluated nuclear data tables to describe the transport of both protons and neutrons at energies up to 150 MeV have recently been made available for an important selection of isotopes [22]. Further modularization of MCNP5 is being accomplished to clarify the logic of transport and the handling of nuclear data in order to allow flexible use of data tables and a variety of physics models. Ultimately, this will enable a seamless treatment of the full particle cascade over a wide range of energies.

8 CONCLUSION

The developmental version of MCNP5 has been enhanced by the addition of several new capabilities to support primary-beam proton transport, making the code a useful tool for simulations in proton radiography. Work is underway to complete the description of the particle cascade to allow future versions of MCNP to address a wide variety of applications in high-energy transport.

9 ACKNOWLEDGMENTS

This work was performed under the auspices of the U. S. Department of Energy by the University of California Los Alamos National Laboratory under contract No. W-7405-Eng-36. Portions of this paper will appear in the proceedings of the ICRS 10 / RPS 2004 meeting, for which we acknowledge Oxford University Press.

10 REFERENCES

1. X-5 Monte Carlo Team, MCNP --- A General Monte Carlo N-Particle Transport Code, Version 5, Volume I: Overview and Theory, Los Alamos Report LA-UR-03-1987 (April 24, 2003).

2. Sternheimer, R. M. and Peierls R. F., "General Expression for the Density Effect for the Ionization Loss of Charged Particles," Phys. Rev. B, 3(11), 3681-3692 (1971).

3. International Commission on Radiation Units and Measurements, Stopping Powers for Electrons and Positrons, ICRU Report 37 (1984).

4. Janni, J. F., "Proton Range-Energy Tables, 1 keV - 10 GeV --- Energy Loss, Range, Path Length, Time-of-Flight, Straggling, Multiple Coulomb Scattering, and Nuclear Interaction Probability," Atomic Data and Nuclear Data Tables, 27, 4/5 (1982).

5. Bichsel, H., "Stopping Power of M Electrons for Heavy Charged Particles," Phys. Rev. A 28, 1147 (1983).

6. Kjandelwal, G., "Shell Corrections for K- and L-Electrons," Nucl. Phys. A 116, 97 (1968).

7. Walske, M., "Stopping Power of K-Electrons," Phys. Rev. 88, 6 (1952).

8. Lindhard, J., "On the Properties of a Gas of Charged Particles," *Kgl. Danske Videnskab. Selskab. Mat.-Fyp. Medd*., **28**, 8 (1954).

9. Armstrong T. W. and Chandler, K. C., SPAR, A FORTRAN Program for Computing Stopping Powers and Ranges for Muons, Charged Pions, Protons, and Heavy Ions, Oak Ridge National Laboratory Report ORNL-4869, (May 1973).

10. Goorley, T., Prael, R. E., and Hughes, H. G., "Verification of Stopping Powers for Proton Transport in MCNP5," Transactions of the American Nuclear Society Winter Meeting, Vol. 88, New Orleans (November 2003).

11. International Commission on Radiation Units and Measurements, *Stopping Powers and Ranges for Protons and Alpha Particles*, ICRU Report 49 (1993).

12. Prael, R. E., and Lichtenstein, H., *User Guide to LCS: The LAHET Code System*, Los Alamos National Laboratory report LA-UR-89-3014 (September 1989).

13. Hughes, H. G., Chadwick, M. B., Corzine, R. K., Egdorf, H. W., Gallmeier, F. X., Little, R. C., MacFarlane, R. E., Mashnik, S. G., Pitcher, E. J., Prael, R. E., Sierk, A. J., Snow, E. C., Waters, L. S., White, M. C., and Young, P. G., "Status of the MCNPX Transport Code," in *Advanced Monte Carlo for Radiation Physics, Particle Transport Simulation and Applications*, Proceedings of the Monte Carlo 2000 Conference, Lisbon, 23-26 October 2000 (Springer, ISBN 3-540-41795-8).

14. Rossi, B., *High-Energy Particles*, Prentice-Hall, Incorporated, New York 1952.

15. Vavilov, P. V., "Ionization Losses of High-Energy Heavy Particles," Soviet Physics JETP 5 (4), 749 (1957).

16. Rotondi, A., and Montagna, P., "Fast Calculation of Vavilov Distribution," Nuclear Instruments and Methods in Physics Research B47, 215 (1990).

17. Striganov, S., "On Theory and Simulation of Multiple Coulomb Scattering of Heavy Particles," to appear in the proceedings of the ICRS 10/RPS 2004, Madeira, Portugal, 9-14 May 2004.

18. Prael, R. E., Liu, L.-C., and Striganov, S., Monte Carlo Model for Proton Elastic Scattering from Optical Model Calculations, Proceedings of the Sixth International Meeting on Nuclear Applications of Accelerator Technology, June 1-5, 2003, San Diego, CA, American Nuclear Society (2003).

19. Barashenkov, V. S. and Polanski, A., "Code for Calculation of Nucleon-Nucleus, Pion-Nucleus and Nucleus-Nucleus Total, Nonelastic and Elastic Cross Sections," *Comm. JINR* **E2** 94-417, Dubna, 1994.

20. Mokhov, N. V., The MARS Code System User's Guide, Fermilab-FN-628 (1995).

21. Mokhov, N. V., *Status of MARS Code*, Fermilab-Conf-03/053 (2003).

22. Chadwick, M. B., Hughes, H. G., Little, R. C., Pitcher, E. J., and Young, P. G., "Nuclear Data for Accelerator-Driven Systems," *Progress in Nuclear Energy* **38 (1/2),** 179 (2001).

23. Berz, M. and Hoefkens, J., COSY INFINITY version 8.1 - programming manual, Technical Report MSUHEP-20703, Department of Physics and Astronomy, Michigan State University, East Lansing, MI 48824 (2002).

24. Gudima, K. K., Mashnik, S. G., and Toneev, V. D., "Cascade-exciton model of nuclear reactions," Nucl. Phys. A401, 329 (1983).

25. Gudima, K. K., Mashnik, S. G., and Sierk, A. J., User Manual for the Code LAQGSM, Los Alamos National Laboratory Report LA-UR-01-6804 (2001).

26. Mashnik, S. G., Sierk, A. J., and Gudima, K. K., "Complex-particle and light-fragment emission in the cascade-exciton model of nuclear reactions," Proceedings of RPSD 2002, Los Alamos National Laboratory Report LA-UR-02-5185 (2002).

27. Mashnik, S. G., Gudima, K. K., and Sierk, A. J., "Merging the CEM2k and LAQGSM codes with GEM2 to describe fission and light-fragment production," *Proceedings of SATIF-6*, Los Alamos National Laboratory Report LA-UR-03-2261 (2003).

28. Baznat, M., Gudima, K., and Mashnik, S., Proton-Induced Fission Cross Section Calculation with the LANL Codes CEM2k+GEM2 and LAQGSM+GEM2, *Proc. AccApp'03*. Los Alamos National Laboratory Report LA-UR-03-3750 (2003).

29. Mashnik, S. G., Gudima, K. K., Sierk, A. J., and Prael, R. E., *Improved Intranuclear Cascade Models for the Codes CEM2k and LAQGSM*, Los Alamos National Laboratory Research Note X-5-RN (U) 04-08, LA-UR-04-0039 (2004).